

# MiSTA: An Age-Optimized Slotted ALOHA Protocol

Mutlu Ahmetoglu, Orhan Tahir Yavascan and Elif Uysal

Dept. of Electrical and Electronics Engineering, METU, 06800, Ankara, Turkey

{mutlu.ahmetoglu,orhan.yavascan,uelif}@metu.edu.tr

## Abstract

We introduce Mini Slotted Threshold-ALOHA (MiSTA), a slotted ALOHA modification designed to minimize the time average Age of Information (AoI) achieved in the network while also increasing throughput. In MiSTA, sources with age below a certain threshold stay silent. Nodes with age above the threshold that decide to transmit test the channel for possible collisions during a mini-slot placed ahead of each data slot. We derive the steady state distribution of the number of active sources and analyze its limiting behaviour. We show that MiSTA probabilistically converges to “thinned” slotted ALOHA, where the number of active users at steady state adjusts to optimize age. With an optimal selection of parameters, the AoI scales with the network size (i.e. the number of sources),  $n$ , as  $0.9641n$ , in contrast to  $1.4169n$  which is the lowest possible scaling with Threshold-ALOHA proposed in earlier literature. While achieving this reduction in age, MiSTA also increases achievable throughput to approximately 53%, from the 37% achievable by Threshold-ALOHA and regular slotted ALOHA.

## Index Terms

Slotted ALOHA, Threshold-ALOHA, Mini Slots, Age of Information, AoI, threshold policy, random access, stabilized ALOHA

## I. INTRODUCTION

Proliferation of IoT, autonomous mobility and remote monitoring applications is influencing the redesign of communication and wireless access protocols to better cater for Machine-Type Communications (MTC). The information timeliness requirements in massive deployments of nodes generating short, sporadic data packets are not captured adequately by conventional

This work was supported in part by TUBITAK grant 119C028, and by Huawei.

protocol principles, based on the main performance metrics throughput and packet delay. The Age of Information (AoI) metric was proposed to more directly capture the timeliness of flows in such applications [1]. Optimization according to AoI leads to non-conventional (and sometimes counter-intuitive) service and scheduling policies [2, 3]. Age optimization has been studied under many network and service models, including random access schemes, leading to suggested innovations at various networking layers [4, 5, 6, 7, 8, 9, 10]. In massive MTC scenarios where nodes are to occasionally send typically short status update packets to a common access point over a shared channel, a simple slotted ALOHA type policy is preferable to scheduled access or even to CSMA-type random access due to the low tolerance for overhead. Accordingly, in recent literature [11, 12, 13, 14, 15, 16] various slotted ALOHA variants protocols have been studied with a focus on the AoI performance. We now briefly review this recent literature to put the present paper into context.

In slotted ALOHA, sources (that are backlogged) transmit with a certain probability  $\tau$  in each slot. The selection of  $\tau$  to minimize time average age was studied in [12]. In [15] it was proposed to activate the transmission with probability  $\tau$  only when a user's age reaches a certain threshold  $\gamma$ , resulting in a policy termed "Threshold ALOHA (TA)". The parameters  $\tau$  and  $\gamma$  were jointly optimized in [11, 17]. Of course, TA depends on feedback at each node about the success of its transmissions, which then exploits to compute age. The benefit of this one bit feedback per successful transmission was shown to be significant, in [11]: the average AoI scales with the network size  $n$  as  $1.4169n$ , in contrast to the best achievable age scaling  $en$  with slotted ALOHA. Moreover, there is nearly no loss in throughput with respect to slotted ALOHA.

The work reported in [14] take the age-based randomized transmission approach to a more detailed dynamic optimization. The SAT policy proposed therein obtains an age-based thinning that is similar to TA except it uses dynamic thresholds resembling a stabilized slotted ALOHA mechanism: sources make decentralized estimations of their ages and compute an age-based transmission threshold, above which they transmit with constant probability. The asymptotic scaling of average AoI with network size, achieved by SAT is slightly better than that achieved by TA:  $en/2 \approx 1.359n$ .

The work to be presented in this paper is also related to the studies in [18] and [19] with respect to its use of reservation slots: In [18], a standard CSMA model with stochastic arrivals was studied for AoI optimization, reaching the conclusion that standard CSMA does not cater well to

age performance. The combined analytical and experimental study reported in [19] also focused on CSMA, in a slotted frame structure. Stochastic arrivals are modeled at the beginning of each frame, which is divided into minislots. Nodes that capture the channel use a certain number of mini slots combined. Sources in this model do not track their ages, and thus make age-oblivious decisions. Analytical results on average AoI obtained by this approach was supported by experimental results from a Software Defined Radio test-bed implementation.

The main contributions of this paper are the following:

- We introduce Mini Slotted Threshold ALOHA (MiSTA) as the following modification of Threshold ALOHA: at the beginning of a slot, each active source (that is, those with ages exceeding  $\Gamma$ ) sends a short beacon signal with probability  $\tau_1$ . If the source receives a collision feedback at the end of this mini-slot, it will back-off with probability  $1 - \tau_2$ . With probability  $\tau_2$ , it will go ahead and transmit a data packet during the remainder of the slot.
- Employing the analysis techniques introduced in [11], we find the explicit steady state solution of the Markov Chain model for the Mini Slotted Threshold ALOHA system, and use it to compute the steady-state distribution of the number of active users for any given network size,  $n$  (Lemma 1).
- We then analyze the asymptotic behaviour of the system as the network size increases. In particular, we establish the independence of the number of active sources and the age of an individual source in the limiting case (Corollary 1). This observation is used as the key ingredient in determining the probability of a successful transmission,  $q_o$ , in steady state.
- We show that in the large network limit, the policy converges to a *thinned* slotted-ALOHA network (i.e. a slotted-ALOHA network with fewer nodes) (Theorem 2 and 3). This resembles the results achieved by Rivest's stabilized slotted ALOHA, or the age-thinning policy introduced in [14].
- We derive an expression for the steady-state time average AoI in terms of  $n$ ,  $\Gamma$ ,  $\tau_1$  and  $\tau_2$ . With the optimal choice of parameters, this expression gives the time average AoI of  $0.9641n$  for the system (Theorem 4). This value was  $1.4169n$  for the Threshold ALOHA policy, which means MiSTA reduces the time average AoI by almost a third. Meanwhile, MiSTA achieves approx. 53% throughput, compared to the 37% achievable by Threshold ALOHA or plain slotted ALOHA.
- We show that, perhaps contrary to immediate intuition, the mini slot introduced by MiSTA

results in no loss in spectral efficiency; on the contrary, a net gain in spectral efficiency. Finally we also numerically present the improved performance achieved by an extended version of MiSTA, including multiple mini slots per slot.

The rest of the paper is organized as follows: In Section II the system model is presented. Our proposed policy, Mini Slotted Threshold-ALOHA (MiSTA) is defined in Section III. Section III-A provides an upper bound for the throughput and a lower bound for the time average AoI attained by MiSTA. In Section III-B the steady state distribution of age under MiSTA for any network size is derived. Section III-C and Section III-D further possible asymptotic steady state behaviours for the system. Section III-E derive age-optimal policy parameters. Section III-F analyzes the spectral efficiency of MiSTA. Section V provides a numerical study to further illustrate MiSTA and its performance. We conclude in section VI with a discussion of possible extensions.

## II. SYSTEM MODEL

We consider a wireless random access channel with  $n$  sources and a single access point (AP). The sources access the AP on a shared channel to send time sensitive status update data to their respective destinations. Any delays from the AP to the destinations is ignored. Time is slotted and all nodes are assumed to be synchronized. Two or more transmissions that occur in the same slot result in a collision where no packet is successfully decoded. We will adopt the “generate-at-will” model [20] where sources take fresh samples of data when they decide to transmit instead of re-transmitting data that failed to be successfully transmitted earlier.

We define  $A_i[t]$  as the Age of Information (AoI) of source  $i \in \{1, \dots, n\}$  at the time slot  $t$ . By its definition,  $A_i[t]$  is the time elapsed since the generation of the most recent successful data transmitted by source  $i$ . In accordance with the generate-at-will model assumption, all received packets reduce the age of the corresponding flow to 1. Hence,  $A_i[t]$  is equal to the the number of slots that have passed by time  $t$  since the latest successful transmission by source  $i$ , plus 1. Building on the structure of Threshold ALOHA [11], we assume one bit feedback per successful transmission, such that the AP informs the successful source in the event of successful decoding. Consequently, the age process evolves as

$$A_i[t] = \begin{cases} 1, & \text{source } i \text{ transmits successfully at time slot } t - 1 \\ A_i[t - 1] + 1, & \text{otherwise} \end{cases} \quad (1)$$

The long term average AoI of source  $i$  is defined as

$$\Delta_i = \lim_{T \rightarrow \infty} \frac{1}{T} \sum_{t=0}^{T-1} A_i[t] \quad (2)$$

whenever the limit exists. In the analysis of threshold ALOHA, the system age vector was constructed with ages of individual sources as

$$\mathbf{A}[t] \triangleq \langle A_1[t] \quad A_2[t] \quad \dots \quad A_n[t] \rangle \quad (3)$$

In [15], it was shown that the evolution of this vector follows a Markov Chain and that a truncated version of this Markov Chain suffices for the analysis of steady-state long term average age in the original model. In this finite state truncated Markov Chain, the source ages are truncated at  $\Gamma$  since the sources behaviour does not change after it becomes active. The truncated Markov Chain has a unique steady-state distribution which is to be determined later in this section. As the sources are symmetric and the Markov Chain is ergodic, the time average AoI can written as:

$$\Delta_i = \lim_{t \rightarrow \infty} \mathbb{E} [A_i[t]] \quad (4)$$

### III. MINI SLOTTED THRESHOLD-ALOHA

MiSTA is a modification of threshold ALOHA where a mini slot is prepended to each slot. The remainder of the slot is of sufficient length for one packet transmission.

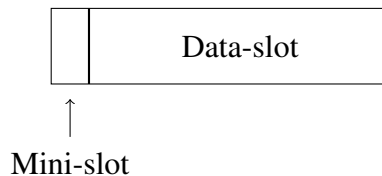


Fig. 1: The slot structure for Mini Slotted Threshold-ALOHA

The mini slots are used by the sources to anticipate interference in the channel before it happens. Before each mini slot, active sources decide to become attempters with probability  $\tau_1$ . During the mini slot attempters transmit their ID information to the AP. If a source receives a success feedback from the access point at the end of the mini slots, it understands that it was the sole attempter and immediately prepares its time sensitive data for transmission in the data slot. On the other hand, if it does not receive the success feedback for its ID transmission, it deduces that there were multiple contenders in this slot. In this case, each attempter independently decides to send data in the rest of the slot with probability  $\tau_2 \leq \tau_1$ . Hence, MiSTA allows nodes

a second chance to avoid collision. Now that we clarified the slot structure we proceed with deriving bounds for both the throughput and the average AoI.

#### A. Lower Bound for Average AoI

It is naturally expected that the average AoI of the system is lower bounded by the throughput of the system. In [14] this intuitive lower bound was derived as the following:

$$\frac{\Delta}{n} \geq \frac{1}{2q^{max}} + \frac{1}{2n} \quad (5)$$

where  $q^{max}$  is the maximum achievable throughput of the system. Since the throughput imposes a limit on the frequency of transmissions, there is a lower bound on AoI which can only be improved by increasing the throughput. Hence, we are motivated to obtain the maximum throughput achievable by MiSTA. As stated earlier,  $\tau_1$  and  $\tau_2$  are the attempt probabilities of the active sources in the beginning of the mini slot and the data slot, respectively. Let the number of active sources be  $m$  in the time slot and  $q$  be the instantaneous throughput of MiSTA. Then  $q$  can be written as:

$$q = m\tau_1(1 - \tau_2)(1 - \tau_1)^{m-1} + m\tau_1\tau_2(1 - \tau_1\tau_2)^{m-1} \quad (6)$$

In our analysis, we mainly focus on the asymptotical case where  $n$  and  $m$  values are large. We define  $G \triangleq m\tau_1$  and rewrite  $q$  in the limit of large  $m$  as:

$$q = \tau_2 G e^{-\tau_2 G} + (1 - \tau_2) G e^{-G} \quad (7)$$

The above expression is optimized with the following choice of parameters:

$$q^{max} = 0.5315, \quad G^* = 1.59, \quad \tau_2^* = 0.38 \quad (8)$$

Finally, we use (5) and (8) to obtain the following proposition.

**Proposition 1.** *Average AoI in MiSTA is lower bounded by  $0.9407n + 0.5$ .*

Since the maximum achievable throughput in slotted ALOHA and TA is  $e^{-1}$ , the age lower bound for these policies is given as  $1.3591n + 0.5$ . Note that the increase in maximum achievable throughput for MiSTA results in an age lower bound which is not obtainable by these policies. In the following subsections, we proceed to asymptotically derive the average AoI expression in steady state.

## B. Steady States of the Markov Chain

In this subsection, we analyze the truncated Markov Chain that is formed with the evolution of the system age vector. Using the steady state probabilities of the recurrent states, we will derive the distribution of the number of active users,  $m$ , as done in [11]. First, we define the truncated system age vector as

$$\mathbf{A}^\Gamma[t] \triangleq \langle A_1^\Gamma[t] \quad A_2^\Gamma[t] \quad \dots \quad A_n^\Gamma[t] \rangle \quad (9)$$

where  $A_i^\Gamma[t] \in \{1, 2, \dots, \Gamma\}$  is the Aol of source  $i$  at time  $t \in \mathbb{Z}^+$  truncated at  $\Gamma$ . The  $A_i^\Gamma[t]$  expression takes the value  $\Gamma$  if the source  $i$  is active in a slot (i.e. if its age is at least  $\Gamma$ ), otherwise  $A_i^\Gamma[t]$  takes the value of the sources age. Therefore, the  $A_i^\Gamma[t]$  expression evolves as:

$$A_i^\Gamma[t+1] = \begin{cases} 1, & \text{src. } i \text{ updates at time } t-1, \\ \min\{A_i^\Gamma[t] + 1, \Gamma\}, & \text{otherwise.} \end{cases} \quad (10)$$

$\{A^\Gamma[t], t \geq 1\}$  is a Markov Chain with a finite state space and a unique steady state distribution, as proved in [15].

**Proposition 2.** *For distinct indices  $i$  and  $j$ , if a state  $\langle s_1 \quad s_2 \quad \dots \quad s_n \rangle$  in the truncated MC  $\{A^\Gamma[t], t \geq 1\}$  is recurrent, then  $s_i = s_j$  if and only if  $s_i = s_j = \Gamma$ .*

*Proof.* The proof can be found in [11]. □

What Prop. 2 essentially means is that states with two equal below-threshold ages are transient. Hence, in recurrent states the only reappearing age value can be  $\Gamma$ . It has been proven that indeed all the states that satisfy Prop. 2 are recurrent. Furthermore, since there is a unique steady state distribution, all these recurrent states are in the same recurrent class. Next, in order to simplify the identification of the recurrent states, we define the *type* of a recurrent state as:

$$T\langle s_1 \quad s_2 \quad \dots \quad s_n \rangle = (M, \{u_1, u_2, \dots, u_{n-M}\}), \quad (11)$$

In this notation,  $M$  is the number of active sources (i.e. sources with the truncated age of  $\Gamma$ ), and the set  $\{u_1, u_2, \dots, u_{n-M}\}$  is the set of age values in the state that correspond to the passive sources (i.e. sources with an age smaller than  $\Gamma$ ). The reason to represent the active sources with their population rather than putting them one by one will be clear later.

**Proposition 3.** *States with the same types have equal steady state probabilities.*

*Proof.* States with the same types can be reached from one another by altering the order of the state entries. Due to the symmetry between the users, modifying the order of the state entries

does not change the steady state probability of a state.  $\square$

Next, we show that the distribution of  $m$ , the number of active sources, in steady state can be derived from the distribution of the Markov Chain. We validate this in lemma 1 by showing that the number  $M$  for a state, which corresponds to the number of active sources pertaining to it, is what determines the steady state probability of that state.

**Lemma 1.** *The following are valid for the truncated Markov Chain  $\{\mathbf{A}^\Gamma[t], t \geq 1\}$ :*

- i)  $M$ , which is the number of active sources given a state vector  $\langle s_1 \ s_2 \ \dots \ s_n \rangle$ , is what solely determines the steady state probability of the state vector.
- ii) Let  $P_m$  be the total steady state probability of states with  $m$  active users. Then the  $\frac{P_m}{P_{m-1}}$  expression is found<sup>1</sup>.

*Proof.* For the proof of Lemma 1, we will define 4 types of state vectors. Let the type 1 be defined as  $\mathcal{T}_1 \triangleq (M, \{u_1, u_2, \dots, u_{n-M}\})$ , where  $M$  is the number of active sources as before and the set  $\{u_1, u_2, \dots, u_{n-M}\}$  contains no entry equal to 1. What this means is that there has not been a successful transmission in the previous slot. Note that there can be at most one entry equal to 1 in the recurrent states, which occurs in the case of successful transmission in the previous slot. Then, the previous slot can be one of two types, type 2 and type 3, defined as

- $\mathcal{T}_2 \triangleq (M, \{u_1 - 1, u_2 - 1, \dots, u_{n-M} - 1\})$
- $\mathcal{T}_3 \triangleq (M - 1, \{\Gamma - 1, u_1 - 1, u_2 - 1, \dots, u_{n-M} - 1\})$

If there was no passive source with the age value  $\Gamma - 1$  in the previous slot, then there must be  $M$  active slots in the previous slot, which is the case represented by type  $\mathcal{T}_2$ . On the other hand, if there was a passive source with the age value  $\Gamma - 1$  in the previous slot, then there must be  $M-1$  active slots in the previous slot since this passive source turns active in this slot, which is the case represented by type  $\mathcal{T}_3$ . The fourth type is defined as  $\mathcal{T}_0 \triangleq (M - 1, \{u_1, u_2, \dots, u_{n-M}, 1\})$  and it represents the case where the previous slot is one of the types  $\mathcal{T}_2$  and  $\mathcal{T}_3$  and it results with a successful transmission. This is why one of the values in the set  $\{u_1, u_2, \dots, u_{n-M}, 1\}$  is equal to 1.

At this point, we see that if the previous slot is one of the types  $\mathcal{T}_2$  and  $\mathcal{T}_3$ , then the present slot can be one of the two types  $\mathcal{T}_0$  and  $\mathcal{T}_1$ . A type  $\mathcal{T}_2$  state precedes a type  $\mathcal{T}_1$  state with probability

<sup>1</sup>The expression is:  

$$\frac{(1 - (m-1)\tau_1(1-\tau_1)^{m-2} - (m-1)\tau_1\tau_2[(1-\tau_1\tau_2)^{m-2} - (1-\tau_1)^{m-2}])(n-m+1)}{(m\tau_1(1-\tau_1)^{m-1} + m\tau_1\tau_2[(1-\tau_1\tau_2)^{m-1} - (1-\tau_1)^{m-1}])(\Gamma-1-n+m)}$$



$1 - M\tau_1(1 - \tau_1)^{M-1} - M\tau_1\tau_2[(1 - \tau_1\tau_2)^{M-1} - (1 - \tau_1)^{M-1}]$  and precedes a type  $\mathcal{T}_0$  state with probability  $\tau_1(1 - \tau_1)^{M-1} + \tau_1\tau_2[(1 - \tau_1\tau_2)^{M-1} - (1 - \tau_1)^{M-1}]$ . A type  $\mathcal{T}_3$  state precedes a type  $\mathcal{T}_1$  state with probability  $M(1 - (M - 1)\tau_1(1 - \tau_1)^{M-2} - (M - 1)\tau_1\tau_2[(1 - \tau_1\tau_2)^{M-2} - (1 - \tau_1)^{M-2}])$  and precedes a type  $\mathcal{T}_0$  state with probability  $(M - 1)\tau_1(1 - \tau_1)^{M-2} - (M - 1)\tau_1\tau_2[(1 - \tau_1\tau_2)^{M-2} - (1 - \tau_1)^{M-2}]$ . If we define  $\pi_{\mathcal{T}_j}$  to be the steady state probability of a state of type  $\mathcal{T}_j$ , we can use the above arguments to write the following equations:

$$\begin{aligned} \pi_{\mathcal{T}_1} = & \pi_{\mathcal{T}_2}(1 - M\tau_1(1 - \tau_1)^{M-1} - M\tau_1\tau_2[(1 - \tau_1\tau_2)^{M-1} - (1 - \tau_1)^{M-1}]) \\ & + \pi_{\mathcal{T}_3}M(1 - (M - 1)\tau_1(1 - \tau_1)^{M-2} - (M - 1)\tau_1\tau_2[(1 - \tau_1\tau_2)^{M-2} - (1 - \tau_1)^{M-2}]) \end{aligned} \quad (12)$$

$$\begin{aligned} \pi_{\mathcal{T}_0} = & \pi_{\mathcal{T}_2}\tau_1(1 - \tau_1)^{M-1} + \tau_1\tau_2[(1 - \tau_1\tau_2)^{M-1} - (1 - \tau_1)^{M-1}] \\ & + \pi_{\mathcal{T}_3}(M - 1)\tau_1(1 - \tau_1)^{M-2} - (M - 1)\tau_1\tau_2[(1 - \tau_1\tau_2)^{M-2} - (1 - \tau_1)^{M-2}] \end{aligned} \quad (13)$$

Since (12) and (13) represent all possible ways of transition between the recurrent states and since the truncated Markov Chain has a unique steady state distribution, this set of equations fully specifies the steady state probabilities. (i) part of the Lemma can be proven here by assigning the probability  $\pi_M$  to the states with  $M$  active sources. With this methodology, it is easy to see that  $\pi_{\mathcal{T}_1} = \pi_{\mathcal{T}_2} = \pi_M$  and  $\pi_{\mathcal{T}_0} = \pi_{\mathcal{T}_3} = \pi_{M-1}$ . If we make the necessary substitutions, (12) becomes:

$$\begin{aligned} \pi_M = & \pi_M(1 - M\tau_1(1 - \tau_1)^{M-1} - M\tau_1\tau_2[(1 - \tau_1\tau_2)^{M-1} - (1 - \tau_1)^{M-1}]) \\ & + \pi_{M-1}M(1 - (M - 1)\tau_1(1 - \tau_1)^{M-2} - (M - 1)\tau_1\tau_2[(1 - \tau_1\tau_2)^{M-2} - (1 - \tau_1)^{M-2}]) \end{aligned} \quad (14)$$

and (13) becomes:

$$\begin{aligned} \pi_{M-1} = & \pi_M\tau_1(1 - \tau_1)^{M-1} + \tau_1\tau_2[(1 - \tau_1\tau_2)^{M-1} - (1 - \tau_1)^{M-1}] \\ & + \pi_{M-1}(M - 1)\tau_1(1 - \tau_1)^{M-2} - (M - 1)\tau_1\tau_2[(1 - \tau_1\tau_2)^{M-2} - (1 - \tau_1)^{M-2}] \end{aligned} \quad (15)$$

If we reduce these equations they turn out to be the same equation that holds for all  $m$ , which is:

$$\frac{\pi_m}{\pi_{m-1}} = \frac{m(1 - (m - 1)\tau_1(1 - \tau_1)^{m-2} - (m - 1)\tau_1\tau_2[(1 - \tau_1\tau_2)^{m-2} - (1 - \tau_1)^{m-2}])}{m\tau_1(1 - \tau_1)^{m-1} + m\tau_1\tau_2[(1 - \tau_1\tau_2)^{m-1} - (1 - \tau_1)^{m-1}]} \quad (16)$$

Then, we have proven that part (i) holds. We will use this to find the total probability of having  $m$  active users in steady state. Due to Prop. 3, the total probability of having  $m$  active sources

in steady state is the number of recurrent states with  $m$  active sources times the probability of one state with  $m$  active sources, which is  $\pi_m$ . The total number of recurrent states with  $m$  active sources is calculated as:

$$N_m = \binom{n}{m} \frac{(\Gamma - 1)!}{(\Gamma - n - 1 + m)!} \quad (17)$$

Then, if we define  $P_m$  to be the total probability of having  $m$  active sources in steady state, we get:

$$P_m = N_m \pi_m \quad (18)$$

$$\frac{P_m}{P_{m-1}} = \frac{(1 - (m-1)\tau_1(1-\tau_1)^{m-2} - (m-1)\tau_1\tau_2[(1-\tau_1\tau_2)^{m-2} - (1-\tau_1)^{m-2}])(n-m+1)}{(m\tau_1(1-\tau_1)^{m-1} + m\tau_1\tau_2[(1-\tau_1\tau_2)^{m-1} - (1-\tau_1)^{m-1}])(\Gamma-1-n+m)} \quad (19)$$

$$\sum_{m=0}^N P_m = 1 \quad (20)$$

From (19) and (20),

$$P_0 \left( 1 + \sum_{m=1}^n \prod_{i=1}^m \frac{(1 - (i-1)\tau_1(1-\tau_1)^{i-2} - (i-1)\tau_1\tau_2[(1-\tau_1\tau_2)^{i-2} - (1-\tau_1)^{i-2}])(n-i+1)}{(i\tau_1(1-\tau_1)^{i-1} + i\tau_1\tau_2[(1-\tau_1\tau_2)^{i-1} - (1-\tau_1)^{i-1}])(\Gamma-1-n+i)} \right) = 1 \quad (21)$$

$$P_m = P_0 \prod_{i=1}^m \frac{(1 - (i-1)\tau_1(1-\tau_1)^{i-2} - (i-1)\tau_1\tau_2[(1-\tau_1\tau_2)^{i-2} - (1-\tau_1)^{i-2}])(n-i+1)}{(i\tau_1(1-\tau_1)^{i-1} + i\tau_1\tau_2[(1-\tau_1\tau_2)^{i-1} - (1-\tau_1)^{i-1}])(\Gamma-1-n+i)} \quad (22)$$

gives the steady state distribution. □

### C. The Analysis of the Pivoted Markov Chain

In this subsection, we will arbitrarily choose a source to be our pivot source without loss of generality, since the sources are symmetric. We will analyze the system through the states of this pivot source by modifying the truncated Markov Chain in the previous subsection  $\{\mathbf{A}^\Gamma[t], t \geq 1\}$ , and obtaining a *pivoted Markov Chain*  $\{\mathbf{P}^\Gamma[t], t \geq 1\}$ . In this pivoted Markov Chain, all the source ages except the pivot source are truncated at  $\Gamma$ . As we did in the previous subsection, we will define the *type* of a state in the pivoted Markov Chain in order to extend the results of Lemma

1 as

$$\mathbf{T}^{\mathbf{P}}\langle S^{\mathbf{P}} \rangle \triangleq (s, M, \{u_1, u_2, \dots, u_{n-M-1}\}) \quad (23)$$

In this new notation,  $s \in \mathbb{Z}^+$  is the state of the pivot source,  $M$  is the number of active sources (i.e. the sources with the entry  $\Gamma$ ) excluding the pivot source, and the set  $\{u_1, u_2, \dots, u_{n-M}\}$  is the set of entries belonging to passive sources (i.e. sources with entry smaller than  $\Gamma$ ), again excluding the pivot source. Similar to the truncated Markov Chain analysis, we will refer to such a state as *type  $M$ -state* where it is clear from the context.

**Proposition 4.** (i)  $\mathbf{P}^{\Gamma}$  has a unique steady state distribution.

(ii) A type- $m$  state in  $\mathbf{P}^{\Gamma}$  has a steady state probability equal to  $\pi_m$ , obeying (16), given that  $s \in \{1, 2, \dots, \Gamma - 1\}$ .

*Proof.* States in  $\mathbf{P}^{\Gamma}$  where  $s = 1, 2, \dots, \Gamma - 1$  correspond to the states in the truncated Markov Chain  $\mathbf{A}^{\Gamma}$  where the source selected as the pivot has the same age. The system visiting these corresponding states in  $\mathbf{P}^{\Gamma}$  and  $\mathbf{A}^{\Gamma}$  is merely the same event, therefore the steady state probabilities and the transition probabilities for these states are equal. Therefore, they follow (16).

Now, for the states in  $\mathbf{P}^{\Gamma}$  for which  $s \geq \Gamma$ , we will prove that steady state probabilities exist. In order to do this, we define a *augmented truncated Markov Chain*  $\{\mathbf{A}^{s,\Gamma}[t], t \geq 1\}$ , in which the only difference with the pivoted Markov Chain is that now the pivot source is truncated at  $s + 1$ . Truncation of the pivot source can be seen in Fig. 2. At this point we consider the state where the state of the pivot source is  $s + 1$  and the state of all the other sources are  $\Gamma$  in the augmented truncated Markov Chain  $\{\mathbf{A}^{s,\Gamma}[t], t \geq 1\}$ . Then we realize that this specified state can be reached by any other state in the augmented truncated Markov Chain including itself, given that none of the last  $s$  consecutive time slots resulted in a successful transmission. This is an event with non-zero probability. Thus, there is a single recurrent class and a unique steady state distribution for the augmented truncated Markov Chain. Finally, since the states in the augmented truncated Markov Chain have one-to-one correspondence with the states in the pivoted Markov Chain, the existence of a unique steady state distribution for the augmented truncated Markov Chain proves the existence of a unique steady state distribution for the states in the pivoted Markov Chain.  $\square$

**Definition 1.** Let the type of a state in  $\mathbf{P}^{\Gamma}$  be defined as  $\mathbf{T}^{\mathbf{P}}\langle S^{\mathbf{P}} \rangle = (s, m, \{u_1, u_2, \dots, u_{n-m-1}\})$  where the  $\{u_i\}$  are ordered from largest to smallest. Let  $Q(S^{\mathbf{P}})$ , preceding type of  $S^{\mathbf{P}}$ , be defined

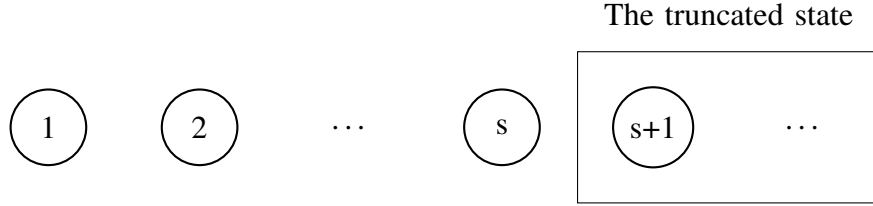


Fig. 2: States of the pivot source in  $\mathbf{A}^{s, \Gamma}$  truncated at  $s + 1$ .

as follows:

$$Q(S^{\mathbf{P}}) = \begin{cases} T^{\mathbf{P}}\langle S^{\mathbf{P}} \rangle, & \text{if } s = 1 \\ (s - 1, m, \{\Gamma - 1, u_1 - 1, u_2 - 1, \dots, u_{n-m-2} - 1\}), & \text{if } s \neq 1, u_{n-m-1} = 1 \\ (s - 1, m, \{u_1 - 1, u_2 - 1, \dots, u_{n-m-1} - 1\}), & \text{if } s \neq 1, u_{n-m-1} \neq 1 \end{cases} \quad (24)$$

As can be seen from its definition,  $Q(S^{\mathbf{P}})$  is defined as the preceding type of  $S^{\mathbf{P}}$  given that the number of active sources (excluding the pivot source),  $m$ , does not change. This reasoning does not hold for the case  $s = 1$ , nonetheless, since this case is not particularly the point of interest, we choose  $Q(S^{\mathbf{P}})$  to be the same type with  $S^{\mathbf{P}}$ . Now that we have covered all possibilities for  $Q(S^{\mathbf{P}})$ , we finally note that we will use  $\pi(S^{\mathbf{P}})$  or  $\pi(s, m, \{u_1, u_2, \dots, u_{n-m-1}\})$  to represent the steady state probability of  $S^{\mathbf{P}}$ .

**Lemma 2.** Choose two arbitrary states in  $\mathbf{P}^{\Gamma}$ ,  $S_1^{\mathbf{P}}$  and  $S_2^{\mathbf{P}}$ , where the state of the pivot source is equal for both states. Let the types of  $S_1^{\mathbf{P}}$  and  $S_2^{\mathbf{P}}$  be:

$$T^{\mathbf{P}}\langle S_1^{\mathbf{P}} \rangle = (s, m_1, \{u_1, u_2, \dots, u_{n-m_1-1}\})$$

$$T^{\mathbf{P}}\langle S_2^{\mathbf{P}} \rangle = (s, m_2, \{v_1, v_2, \dots, v_{n-m_2-1}\})$$

i) Let  $Q_1^{\mathbf{P}}$  be any state satisfying  $T^{\mathbf{P}}\langle Q_1^{\mathbf{P}} \rangle = Q(S_1^{\mathbf{P}})$ . Then,

$$\lim_{n \rightarrow \infty} \frac{\pi(S_1^{\mathbf{P}})}{\pi(Q_1^{\mathbf{P}})} = 1 \quad (25)$$

ii) If  $m_1 = m_2$ , then

$$\lim_{n \rightarrow \infty} \frac{\pi(S_1^{\mathbf{P}})}{\pi(S_2^{\mathbf{P}})} = 1 \quad (26)$$

iii) If  $m_1 = m_2 + 1$ , then

$$\lim_{n \rightarrow \infty} \frac{\pi(S_1^{\mathbf{P}})}{n \pi(S_2^{\mathbf{P}})} = \frac{1}{\alpha e^{-k\alpha} + \alpha \tau_2 (e^{-\tau_2 k \alpha} - e^{-k\alpha})} - k \quad (27)$$

where  $\lim_{n \rightarrow \infty} \frac{m_1}{n} = k$  and  $\lim_{n \rightarrow \infty} \tau_1 n = \alpha$ . ( $k, \alpha \in \mathbb{R}^+$ )

*Proof.* See Appendix A. □

**Theorem 1.** For some  $r, \alpha \in \mathbb{R}^+$ , such that  $\lim_{n \rightarrow \infty} \frac{\Gamma}{n} = r$  and  $\lim_{n \rightarrow \infty} \tau_1 n = \alpha$ , define  $f : (0, 1) \rightarrow \mathbb{R}$ :

$$f(x) = \ln\left(\frac{1}{x\alpha e^{-x\alpha} + x\alpha\tau_2(e^{-\tau_2 x\alpha} - e^{-x\alpha})} - 1\right) + \ln\left(\frac{r}{x + r - 1} - 1\right) \quad (28)$$

Then, for all  $m$  such that  $\lim_{n \rightarrow \infty} \frac{m}{n} = k \in (0, 1)$  and  $s \in \mathbb{Z}^+$

$$\lim_{n \rightarrow \infty} \ln \frac{P_m^{(s)}}{P_{m-1}^{(s)}} = f(k) \quad (29)$$

where  $P_m^{(s)}$  is the steady state probability of having  $m$  active sources (excluding the pivot source), where state of the pivot source is  $s$ .

*Proof.* The total steady state probability of the states with  $m$  active sources where the pivot source is in the state  $s$  is  $P_m^{(s)}$ . The total number of such states is given as:

$$N_m = \binom{n-1}{m} \frac{(\Gamma-1)!}{(\Gamma-n+m)!} \quad (30)$$

Likewise, the total number of states with  $m-1$  active sources where the pivot source is in the state  $s$  is:

$$N_{m-1} = \binom{n-1}{m-1} \frac{(\Gamma-1)!}{(\Gamma-n+m-1)!} \quad (31)$$

Then, the following gives the desired result

$$\begin{aligned} \lim_{n \rightarrow \infty} \frac{P_m^{(s)}}{P_{m-1}^{(s)}} &= \lim_{n \rightarrow \infty} \frac{\sum_{i=1}^{N_m} \pi(S_i^{(m)})}{\sum_{j=1}^{N_{m-1}} \pi(S_j^{(m-1)})} \\ &\stackrel{(a)}{=} \lim_{n \rightarrow \infty} \frac{n \sum_{i=1}^{N_m} \left[ \pi(S_i^{(m)}) / n\pi(S_1^{(m-1)}) \right]}{\sum_{j=1}^{N_{m-1}} \left[ \pi(S_j^{(m-1)}) / \pi(S_1^{(m-1)}) \right]} \stackrel{(b)}{=} \lim_{n \rightarrow \infty} \frac{n \sum_{i=1}^{N_m} \left( \frac{1}{\alpha e^{-k\alpha} + \alpha\tau_2(e^{-\tau_2 k\alpha} - e^{-k\alpha})} - k \right)}{\sum_{j=1}^{N_{m-1}} 1} \\ &= \lim_{n \rightarrow \infty} \frac{n N_m \left( \frac{1}{\alpha e^{-k\alpha} + \alpha\tau_2(e^{-\tau_2 k\alpha} - e^{-k\alpha})} - k \right)}{N_{m-1}} \\ &= \lim_{n \rightarrow \infty} \frac{n(n-m) \left( \frac{1}{\alpha e^{-k\alpha} + \alpha\tau_2(e^{-\tau_2 k\alpha} - e^{-k\alpha})} - k \right)}{m(\Gamma-n+m)} \\ &= \left( \frac{1}{k\alpha e^{-k\alpha} + k\alpha\tau_2(e^{-\tau_2 k\alpha} - e^{-k\alpha})} - 1 \right) \left( \frac{1-k}{r+k-1} \right) \end{aligned} \quad (32)$$

where in the (a) step both sides of the fraction are divided to the steady state probability of a state with  $m-1$  active sources where the pivot source is in the state  $s$ , and (b) follows from Lemma 2 (ii) and (iii). Hence,

$$\lim_{n \rightarrow \infty} \ln \frac{P_m^{(s)}}{P_{m-1}^{(s)}} = \ln\left(\frac{1}{k\alpha e^{-k\alpha} + k\alpha\tau_2(e^{-\tau_2 k\alpha} - e^{-k\alpha})} - 1\right) + \ln\left(\frac{r}{r+k-1} - 1\right) = f(k) \quad (33)$$

□

What we essentially discovered is that as  $n \rightarrow \infty$ , the relation  $P_m^{(s)}/P_{m-1}^{(s)}$  solely determines the distribution of  $m$ , no matter what the  $s$  value is. This means that the number of active sources excluding the pivot source,  $m$ , is independent of the state of the pivot source. This result is formally expressed in the following corollary:

**Corollary 1.** *In the limit of a large network ( $n \rightarrow \infty$ ),*

- (i) *The number of active sources,  $m$ , (excluding the pivot) and the state of the pivot source,  $s$ , are independent.*
- (ii) *Given that the pivot source is active (i.e.  $s \geq \Gamma$ ),  $\tau_1(1 - \tau_1)^{m-1} + \tau_1\tau_2[(1 - \tau_1\tau_2)^{m-1} - (1 - \tau_1)^{m-1}]$  is the probability of a successful transmission being made by the pivot source which has no dependence on  $s$ .*
- (iii) *The probability of the pivot state being reset to 1 given that the pivot is active is  $q_s = \lim_{l \rightarrow \infty} \sum_{m=0}^l P_m^{(s)}(\tau_1(1 - \tau_1)^{m-1} + \tau_1\tau_2[(1 - \tau_1\tau_2)^{m-1} - (1 - \tau_1)^{m-1}])$ .*

*Proof.* Parts (i) and (ii) follow from the proof of Lemma 1. Since the distribution of the number of active sources  $m$  and the state of the active source  $s$  are independent, no matter what the  $s$  value is, the pivot source observes the same number of active sources. Hence, the transition probabilities from  $s = i$  to  $s = i + 1$  for  $i < \Gamma$ , and the transition probability from  $s \geq \Gamma$  to 1 depends only on the number of active users. This means the evolution of the pivot source state  $s$  is like shown in Fig. 3. □

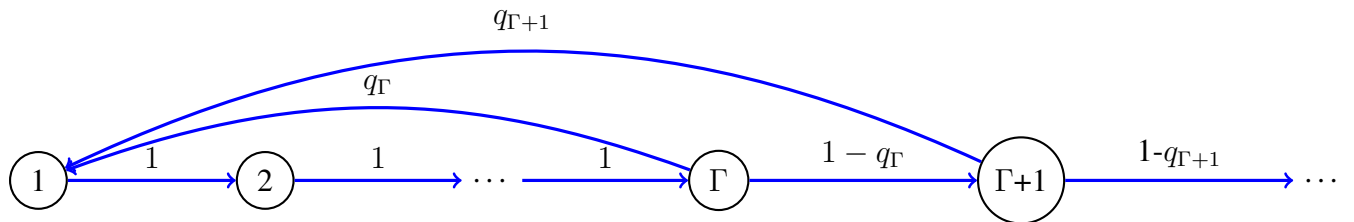


Fig. 3: State diagram of the pivot source

The transitions to the state 1 in Fig. 3 represent successful transmissions made by the pivot source. In the rest, we will consider the asymptotic case of a large network as  $n$  grows. All the transition probabilities to 1 (i.e. all the successful transmissions of the pivot source) will have the same probability  $q_o$  when  $n \rightarrow \infty$ , which will be showed later.

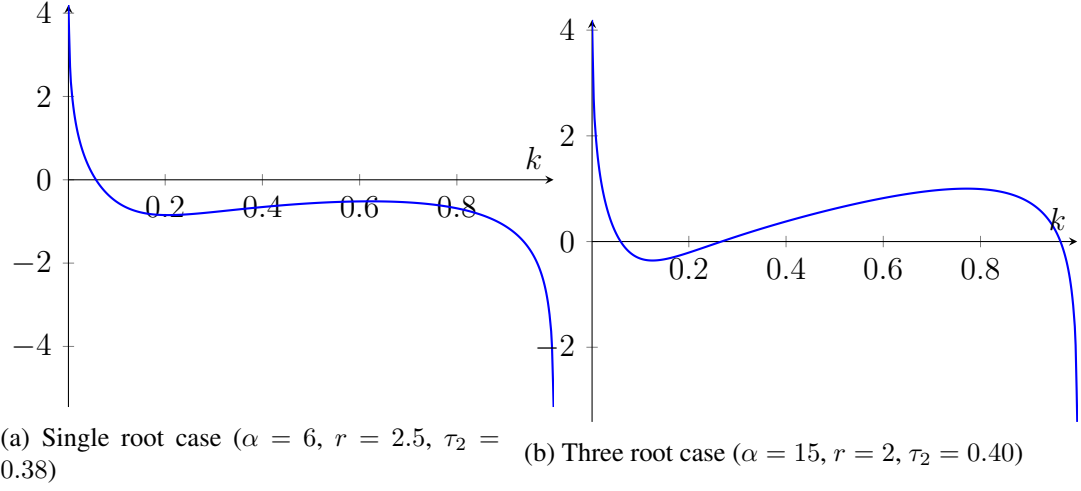


Fig. 4: Plot of  $f(k)$

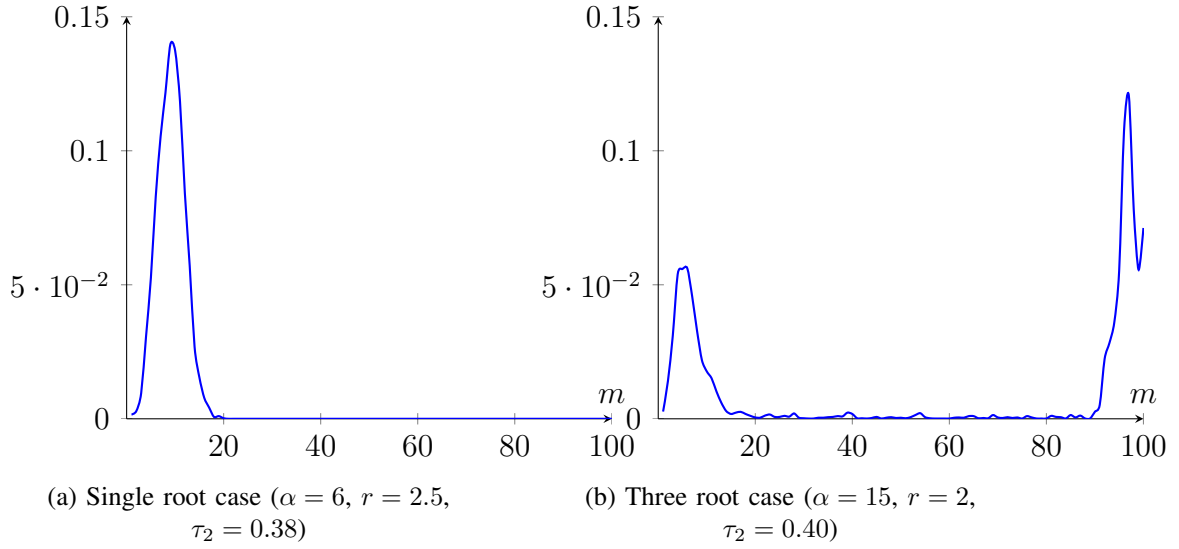


Fig. 5: PMF of  $m$  ( $n = 100$ )

#### D. Large Network Asymptotics

In this subsection, we examine the asymptotic behaviour of  $m$ , and find its PMF as  $n \rightarrow \infty$ . We investigate the properties of the function  $f$  of Theorem 1, since it provides valuable insight on the distribution of  $m$ . With this methodology, we prove that the fraction of active sources,  $k$ , converges to the root of  $f$  in probability.

We replace some parameters of the model,  $\tau_1$  and  $\Gamma$  in the asymptotic analysis. Instead of these parameters, we use the following ones which control their scaling with  $n$ . Due to its definition, the fraction of active users,  $k$ , will take values between 0 and 1.

$$\alpha = n\tau_1, \quad r = \Gamma/n, \quad k = m/n \quad (34)$$

In this setting,  $k$  is the variable of the system while  $\alpha, r$  and  $\tau_2$  are fixed parameters. The

value  $k$  is by its definition proportional to the instantaneous system load. The use of the  $f(k)$  function at this point is due to the fact that roots of this function correspond to the local extrema of  $P_m$ . Specifically, decreasing roots of  $f(k)$  correspond to the local maxima of  $P_m$ , where both  $\ln P_m/P_{m-1}$  and  $\ln P_m/P_{m+1}$  are positive.

Then, the number of roots  $f(k)$  has is what restricts the number of local maxima for  $P_m$ . When the system was run using combinations of system parameters, it was observed that  $f(k)$  may have more than 3 roots. Nevertheless, for more than 3 roots the AoI performance of the system is poor compared to 1 or 3 roots. Thus, in our analysis we consider these two cases with desirable AoI results, which correspond to one local maximum and two local maxima for  $P_m$ , respectively. Despite their similarity, we analyze these cases apart starting with one local maximum, presented in 2.

**Theorem 2.** *Let  $m$  be the number of active sources and  $k_0$  be the only root of  $f(k)$ . For the sequence  $\epsilon_n = cn^{-1/3}$  where  $c \in \mathbb{R}^+$ ,*

$$\Pr\left(\left|\frac{m}{n} - k_0\right| < \epsilon_n\right) \rightarrow 1 \quad (35)$$

*Proof.* The proof can be found in [11]. □

The essential result of this theorem is that MiSTA converges to a thinned slotted-ALOHA policy, where only  $nk$  sources are active at each slot. Since the fraction of active sources  $k$  converges to  $k_0$ , this thinned slotted-ALOHA scheme has exactly  $nk_0$  active sources at each slot, independent of individual states of the sources. This reduction in the number of contenders for a slot decreases the chance for interference and thus results in better throughput and AoI performance.

Now, we analyze the two local maxima case. Theorem 3 very much resembles Theorem 2, however, it has an additional integral constraint to be applicable.

The difference between one local maximum and two local maxima cases is that in the two local maxima case, there are two decreasing roots of  $f(k)$  that  $k$  may converge to, which are the smallest and largest roots. As presented in Theorem 3, the one that  $k$  actually converges in probability is determined by the sign of the integral of  $f(k)$  between these two roots.

**Theorem 3.** *Let  $k_0, k_1, k_2$  be three distinct roots of  $f(k)$  in increasing order and  $m$  be the number of active sources.*



i) If the integral of  $f$  taken from  $k_0$  to  $k_2$  is negative, then for the sequence  $\epsilon_n = cn^{-1/3}$  where  $c \in \mathbb{R}^+$ ,

$$\Pr\left(\left|\frac{m}{n} - k_0\right| < \epsilon_n\right) \rightarrow 1 \quad (36)$$

ii) If the integral of  $f$  taken from  $k_0$  to  $k_2$  is positive, then for the sequence  $\epsilon_n = cn^{-1/3}$  where  $c \in \mathbb{R}^+$ ,

$$\Pr\left(\left|\frac{m}{n} - k_2\right| < \epsilon_n\right) \rightarrow 1 \quad (37)$$

*Proof.* The proof can be found in [11]. □

Since we desire  $k$  to converge to  $k_0$ , so that the number of active sources is the smallest possible, the system parameters should be selected accordingly. Although the two local maxima case yields similar results with the single local maximum case, there are some drawbacks regarding the former. In networks with fewer number of users, steady state probabilities may not converge fast enough to yield the desired results, which may result in congestions due to excess active sources. Consequently, the benefits of our policy requires that this case is avoided. Single root case does not have this drawback and approaches the theoretical value more quickly. Another problem that may arise is that in networks with large number of users, poor selection of initial conditions may lead to undesired results. If all the sources are initially active, the aforementioned congestion scenarios occur, making the convergence in Theorem 3 impossible in a reasonable time. In order to avoid such problems, the initial states of the sources may be randomly selected.

Although it has some drawbacks, the two local maxima case provides asymptotically optimal results and it is preferable for large networks.

#### *E. Steady State Average AoI in the Large Network Limit*

**Theorem 4.** *In the large network limit (i.e.  $n \rightarrow \infty$ ), optimal parameters of MiSTA satisfy the following:*

$$\lim_{n \rightarrow \infty} \frac{\Gamma^*}{n} = 1.59 \quad (38)$$

$$\lim_{n \rightarrow \infty} n\tau_1^* = 10 \quad (39)$$

$$\tau_2^* = 0.38 \quad (40)$$

Furthermore, the optimal expected AoI at steady state scales with  $n$  as:

$$\lim_{n \rightarrow \infty} \frac{\Delta^*}{n} = 0.9641 \quad (41)$$

*Proof.* At the ending of section III-C,  $q_0$  was defined as the successful transmission probability of an active source, moreover, it has been argued that this value is fixed, or independent of age, in the steady state as the number of active sources converge to a value. We can also express  $q_0$  in the following way:

$$q_0 = \mathbb{E}[\tau_1(1 - \tau_1)^{M-1} + \tau_1\tau_2[(1 - \tau_1\tau_2)^{M-1} - (1 - \tau_1)^{M-1}]] \quad (42)$$

where the expectation is over the PMF of the number of active sources,  $M$ , at steady state, which was analyzed earlier. We will first prove that

$$\lim_{n \rightarrow \infty} n q_0 = \alpha e^{-k_0\alpha} + \alpha\tau_2(e^{-\tau_2 k_0\alpha} - e^{-k_0\alpha}) \quad (43)$$

Let  $\gamma_n$  be defined as:

$$\gamma_n \triangleq \Pr(m_0 - cn^{2/3} < M < m_0 + cn^{2/3}) \quad (44)$$

where  $m_0 = k_0n$ . From Theorems 2 and 3,  $\gamma_n \rightarrow 1$  as  $n \rightarrow \infty$ . When  $M$  satisfies the bounds given in (44), the successful transmission probability,  $q_0$ , is also bounded. With this information, the following bound on  $q_0$  is found:

$$\gamma_n[(\tau_1(1 - \tau_1)^{m_0} + \tau_1\tau_2[(1 - \tau_1\tau_2)^{m_0} - (1 - \tau_1)^{m_0}])(1 - \tau_1)^{-cn^{2/3}}] < q_0 \quad (45)$$

$$q_0 < \gamma_n[(\tau_1(1 - \tau_1)^{m_0} + \tau_1\tau_2[(1 - \tau_1\tau_2)^{m_0} - (1 - \tau_1)^{m_0}])(1 - \tau_1)^{cn^{2/3}}] + (1 - \gamma_n)$$

As  $n \rightarrow \infty$ , both upper and lower bounds converge to  $\tau_1(1 - \tau_1)^{m_0} + \tau_1\tau_2[(1 - \tau_1\tau_2)^{m_0} - (1 - \tau_1)^{m_0}]$ .

Finally,

$$\lim_{n \rightarrow \infty} n q_0 = \lim_{n \rightarrow \infty} n\tau_1(1 - \tau_1)^{m_0} + n\tau_1\tau_2[(1 - \tau_1\tau_2)^{m_0} - (1 - \tau_1)^{m_0}] = \alpha e^{-k_0\alpha} + \alpha\tau_2(e^{-\tau_2 k_0\alpha} - e^{-k_0\alpha}) \quad (46)$$

Since the transitions between the states of a source is as given in Fig. 3, value of  $q_0$  can be used to compute the steady state probabilities of the states. Furthermore, the states correspond one-to-one with the ages the source have. Then, finding the steady state probabilities of the states is merely finding the steady state probabilities of the ages. With this methodology, the steady state probability of state  $j$  is:

$$\pi_j = \frac{(1 - q_0)^{\max\{j-\Gamma, 0\}}}{\Gamma - 1 + 1/q_0}, \quad j = 1, 2, \dots \quad (47)$$

The expected time-average AoI expression is found using the steady state probabilities of the ages:

$$\Delta = \frac{\Gamma(\Gamma - 1)}{2(\Gamma - 1 + 1/q_0)} + 1/q_0 \quad (48)$$

The average AoI is also expressed in the limit of large network as:

$$\lim_{n \rightarrow \infty} \frac{\Delta}{n} = \frac{r^2}{2(r + \frac{1}{\alpha e^{-k_0 \alpha} + \alpha \tau_2 (e^{-\tau_2 k_0 \alpha} - e^{-k_0 \alpha})})} + \frac{1}{\alpha e^{-k_0 \alpha} + \alpha \tau_2 (e^{-\tau_2 k_0 \alpha} - e^{-k_0 \alpha})} \quad (49)$$

The system parameters  $r$  and  $k_0$  can be used to re-express(49) as:

$$\lim_{n \rightarrow \infty} \frac{\Delta}{n} = r \frac{k_0^2 + 1}{2(1 - k_0)} \quad (50)$$

With the right selection of system parameters, the Average AoI expression can be minimized.  $\square$

Analyzing (49), optimal parameters and some other steady-state characteristics such as  $k_0$  and average AoI, are derived for MiSTA. These findings are provided in Table I with corresponding values for threshold-ALOHA and slotted-ALOHA for comparison. Since both threshold-ALOHA and MiSTA have two regimes of operation, namely two local maxima case and single local maximum case, the results for these regimes are provided separately.

As presented in Table I, the average AoI value drops to nearly half this value in threshold-ALOHA policy, while approximately maintaining the throughput level of slotted-ALOHA. MiSTA policy we propose in this paper, on the other hand, significantly increases the throughput value and decreases the average AoI to an even smaller value.

	$r^*$	$\alpha^*$	$\tau_2^*$	$k_0^*$	$\Delta^*/n$	$Thr.$
MiSTA(SP)	1.59	9.8	0.37	0.1565	0.9656	0.5252
MiSTA(DP)	1.59	10	0.38	0.1555	<b>0.9641</b>	0.5266
TA(SP)	2.17	4.43	—	0.2052	1.4226	0.3658
TA(DP)	2.21	4.69	—	0.1915	<b>1.4169</b>	0.3644
SA	0	1	—	1	$e$	$e^{-1}$

TABLE I: A comparison of optimized parameters of ordinary slotted ALOHA, threshold-ALOHA and mini slotted threshold-ALOHA and the resulting AoI and throughput values.  $r^*$ : age-threshold/ $n$ ;  $\tau_2^*$ : probability of transmission in the second toss;  $\alpha^*$ : transmission probability $\times n$ ;  $k_0^*$ : expected fraction of active users;  $\Delta^*$ : avg. AoI

#### F. Spectral Efficiency of Mini Slotted Threshold-ALOHA

When we propose prepending a mini slot to each data slot, one of the first concerns is to conserve the spectral efficiency of the system. Hence, in this section we present that contrary

to the immediate intuition MiSTA increases the spectral efficiency of the system, especially for large data slots. The reason for the improvement is that spectral efficiency lost in mini slots is compensated by the increase in the throughput value. Now, we will present these results formally using the notation in Table II.

$\eta$	Spectral efficiency of the threshold-ALOHA(bits/s/Hz)
$\eta'$	Spectral efficiency of the mini slotted threshold-ALOHA (bits/s/Hz)
$B$	Channel Bandwidth
$H$	Time Horizon
$T_b$	The time it takes to send 1 bit (s)
$\theta_1$	Throughput of threshold-ALOHA
$\theta_2$	Throughput of mini-slotted threshold-ALOHA
$c$	Number of bits in the data slot
$d$	Number of bits in the mini slot

TABLE II: Notation table for the symbols relating to spectral analysis

With the definitions given Table II, we first derive the following expressions.

$$\eta = \frac{H\theta_1 c}{HBcT_b} = \frac{\theta_1}{BT_b} \quad (51)$$

$$\eta' = \frac{H\theta_2 c}{HB(c+d)T_b} = \frac{\theta_2 c}{(c+d)BT_b} \quad (52)$$

$$\frac{\eta'}{\eta} = \frac{\theta_2}{\theta_1} \frac{c}{c+d} \quad (53)$$

In order to preserve the spectral efficiency, the  $\eta/\eta'$  expression should at least be equal to 1.

The typical values the  $\theta_2/\theta_1$  expression takes are given in Table II.

	MiSTA( $\theta_2$ )	TA( $\theta_1$ )	$\theta_2/\theta_1$
1000 Sources	0.5251	0.3632	1.448
500 Sources	0.5179	0.3581	1.446
100 Sources	0.5019	0.3633	1.382

TABLE III: Typical values the  $\theta_2/\theta_1$  expression takes for three different  $n$  values, for both the mini slotted threshold-ALOHA and threshold-ALOHA

With the typical values of  $\theta_2/\theta_1$  given in Table III, we see that as long as the  $c/d$  expression is greater than 2.23, there is no loss of spectral efficiency in MiSTA policy.

In the protocols which are currently used in real time systems such as IEEE 802.11, the  $c$  value is typically a few kbytes. Moreover, for the identification purposes of the mini slot 128 bits is adequate for the  $d$  value. Hence, even for a  $c$  value of 2 kbytes  $c/d$  value greatly exceeds 2.23, which shows that mini slots do not result in a loss of spectral efficiency. In fact, MiSTA outperforms threshold-ALOHA regarding the spectral efficiency.

#### IV. A FURTHER EXTENSION: MULTIPLE MINI SLOTTED THRESHOLD-ALOHA

A further extension of MiSTA that naturally comes to mind is a so called *Multiple Mini Slotted Threshold-ALOHA (MuMiSTA)* policy, where a multiple number of mini slots are prepended at each slot. Such a policy achieves a throughput value of 95% with just 32 mini slots. Subsequently, the average AoI scales with  $n$  as  $0.531n$ . The simulation results for MuMiSTA policy are presented in Fig. 6 together with the simulation results of [19] for comparison. In these simulations MuMiSTA is run for  $10^7$  with 32 mini slots and 100 users. It is apparent that this protocol becomes even more efficient when data slots become noticeably longer than mini slots.

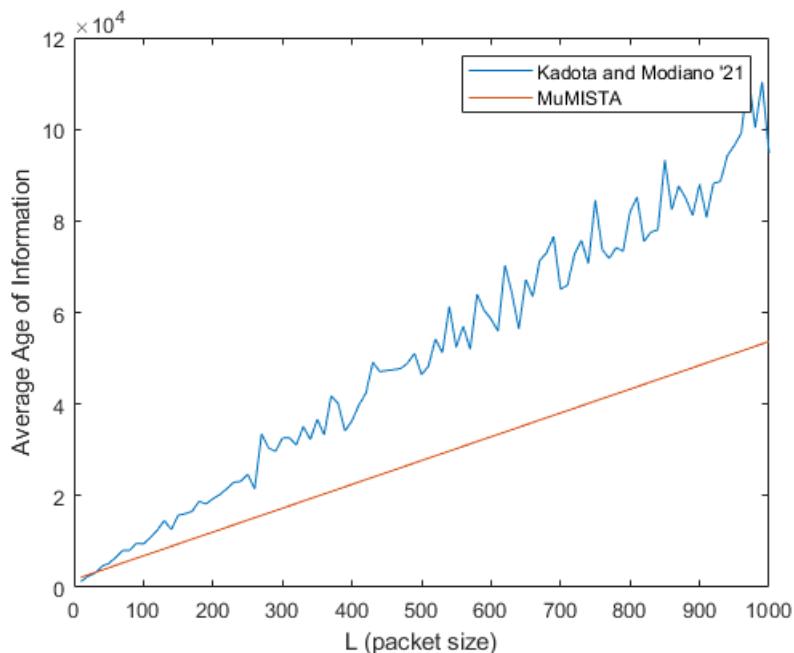


Fig. 6: Comparison of MuMiSTA and the reservation based random access policy in [19].

## V. NUMERICAL RESULTS AND DISCUSSION

In this section, we provide numerical analysis done with simulations that verify the analytical results derived. In addition, we provide the numerical results with the same simulation method for slotted-ALOHA and threshold-ALOHA for comparison. In these simulations, the number of sources ranges between 50 and 1000, the system is run for  $10^7$  time slots and the initial states of the sources are randomized in order to prevent initial congestion. First we compare the AoI performances of these policies in Fig. 7, where AoI is plotted against  $n$ . As expected, threshold-ALOHA reduces the minimum AoI achievable by slotted-ALOHA to almost one half, while MiSTA outperforms both by reducing this value to roughly one third of achievable by slotted-ALOHA. Then, we plot the throughput results for these policies in Fig. 8, again plotting against  $n$ . As was the case for AoI performance, numerical results for throughput are matching the findings in Table I, where we had found that MiSTA increases the throughput to roughly 53%.

As these results verify, the addition of mini slot functionality to the threshold-ALOHA had cut the fraction of sources which are active for large  $n$  to 15%, which increased the throughput value by 45%, decreased the minimum AoI achievable from  $1.4169n$  to  $0.9641n$ , which is a difference that is more and more significant as  $n$  grows, and finally increased the spectral efficiency in all practical cases.

In CSMA type policies, the nodes choose a random back-off time from a contention window after a successful transmission. When a transmission is detected the back-off counter is frozen and also after each collision the contention window widens exponentially. In comparison, we see that in MiSTA the age threshold  $\Gamma$  is the initial stage of a back-off time after a successful transmission and its duration is constant. After the node becomes active again, the time it waits until its next successful transmission is the second part of our back-off time, which is geometrically distributed. Furthermore, the ID sending and feedback receiving function of the mini slot very much resembles the RTS/CTS mechanism in CSMA. Hence, the functionality of the mini slot resembles the carrier sense mechanism in a manner that nodes check the channel for possible contenders before transmission and the back-off schedules of two policies have similar probabilistic distributions. These observations mean that further work may reveal more common ground between two policies.

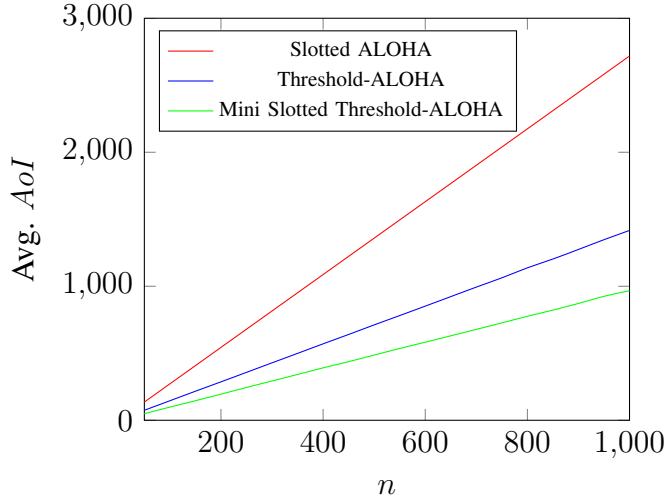


Fig. 7: Optimal time average  $AoI$  vs  $n$ , number of sources, under Slotted ALOHA (computed), threshold-ALOHA (simulated) and mini slotted threshold-ALOHA (simulated).

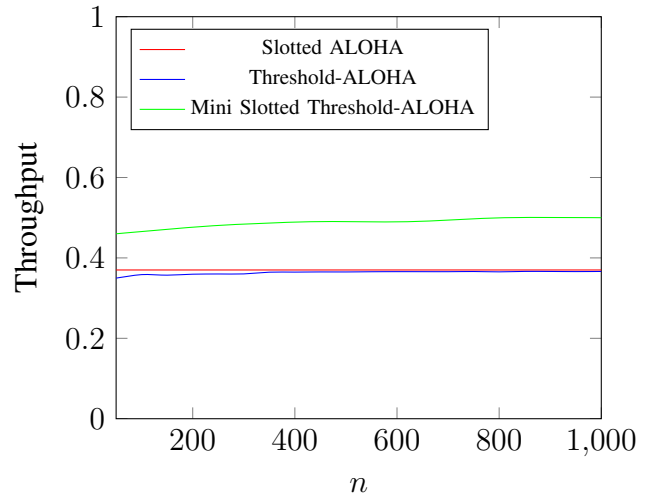


Fig. 8: Throughput vs  $n$ , number of sources, under Slotted ALOHA (computed), threshold-ALOHA (simulated) and mini slotted threshold-ALOHA (simulated).

## VI. CONCLUSION

In this paper, we propose a novel modification for threshold-ALOHA policy which is called *Mini Slotted Threshold-ALOHA (MiSTA)*. The novelty that MiSTA brings about on top of Threshold-ALOHA is the change in slot structure, where instead of having homogeneous blocks of time we have a mini slot prepended to the data slots. We clarified the functionality of the mini slots and the general flow of the system. We modeled this system with a truncated Markov Chain constructed with the ages of the individual sources, then found the steady state distribution of this Markov Chain. Using this steady state distribution and an arbitrary source selected as a pivot, we derived an  $AoI$  expression with the defined system parameters. We found and presented in Table I the optimal system parameters that result in minimal  $AoI$  for a large network size. The results show that MiSTA is equivalent to a thinned slotted-ALOHA with around 15% of all sources active at a slot and it has an optimal  $AoI$  value of  $0.9641n$ , which is scaled with  $n$ . When compared, the minimum achievable  $AoI$  with MiSTA is around one third of that achievable by plain slotted-ALOHA. In addition to its  $AoI$  performance, MiSTA increases the throughput value of slotted-ALOHA by approximately 45% and increases the spectral efficiency of the system in all practical cases.

For future work, the *MuMiSTA* policy briefly defined and numerically presented in this paper can be formally modeled and analyzed. Furthermore, different scenarios for the MiSTA policy

can be analyzed, such as stochastic arrivals, unreliable channels or contention resolution methods [21] where multiple transmissions are permitted in a slot .

## APPENDIX A

### PROOF OF LEMMA 2

We will begin the proof for the  $s$  values  $s = 1, 2, \dots, \Gamma - 1$ . The properties (i) and (ii) directly follow from Prop. 4 (i), where  $\pi(S_1^{\mathbf{P}}) = \pi_{m_1}$  and  $\pi(S_2^{\mathbf{P}}) = \pi_{m_2}$ . Although Property (iii) follows from the same property, it is not directly seen:

$$\begin{aligned} \lim_{n \rightarrow \infty} \frac{\pi(S_1^{\mathbf{P}})}{n \pi(S_2^{\mathbf{P}})} &= \lim_{n \rightarrow \infty} \frac{\pi_{m_1}}{n \pi_{m_1-1}} \\ &\stackrel{(a)}{=} \lim_{n \rightarrow \infty} \frac{(1 - (m_1 - 1)\tau_1(1 - \tau_1)^{m_1-2} - (m_1 - 1)\tau_1\tau_2[(1 - \tau_1\tau_2)^{m_1-2} - (1 - \tau_1)^{m_1-2}])}{n\tau_1(1 - \tau_1)^{m_1-1} + n\tau_1\tau_2[(1 - \tau_1\tau_2)^{m_1-1} - (1 - \tau_1)^{m_1-1}]} \\ &= \frac{1}{\alpha e^{-k\alpha} + \alpha\tau_2(e^{-\tau_2 k\alpha} - e^{-k\alpha})} - k \end{aligned} \quad (54)$$

where the step (a) follows from (16).

Next, we move on to the  $s$  value  $s = \Gamma$  and show that the properties still hold. We will start with showing that  $\pi(S_1^{\mathbf{P}}) = \pi_{m_1}$ . Assuming that  $1 \notin \{u_1, u_2, \dots, u_{n-m_1-1}\}$  holds and  $S_1^{\mathbf{P}}$  is the current state, the previous state can be one of the following types:

- $(\Gamma - 1, m_1, \{u_1 - 1, u_2 - 1, \dots, u_{n-m_1-1} - 1\})$
- $(\Gamma - 1, m_1 - 1, \{\Gamma - 1, u_1 - 1, u_2 - 1, \dots, u_{n-m_1-1} - 1\})$

In Prop. 4 (ii), the steady state probabilities of these types are given as  $\pi_{m_1}$  and  $\pi_{m_1-1}$ , respectively. The steady state probability of  $S_1^{\mathbf{P}}$  can be calculated using the given probabilities for the preceding state and their transition probabilities as:

$$\begin{aligned} \pi(S_1^{\mathbf{P}}) &= \pi_{m_1}(1 - m_1\tau_1(1 - \tau_1)^{m_1-1} - m_1\tau_1\tau_2[(1 - \tau_1\tau_2)^{m_1-1} - (1 - \tau_1)^{m_1-1}]) \\ &\quad + \pi_{m_1-1}m_1(1 - (m_1 - 1)\tau_1(1 - \tau_1)^{m_1-2} - (m_1 - 1)\tau_1\tau_2[(1 - \tau_1\tau_2)^{m_1-2} - (1 - \tau_1)^{m_1-2}]) \\ &= \pi_{m_1} \end{aligned} \quad (55)$$

where the  $\pi_{m_1}$  result is obtained through the ratio given in (16). Now that we are done with the case of  $1 \notin \{u_1, u_2, \dots, u_{n-m_1-1}\}$ , we move on to the case  $1 \in \{u_1, u_2, \dots, u_{n-m_1-1}\}$ . We will assume  $u_{n-m_1-1} = 1$  without loss of generality and then follow similar steps with the preceding case. The previous state can be one of the following this time:

- $(\Gamma - 1, m_1 + 1, \{u_1 - 1, u_2 - 1, \dots, u_{n-m_1-2} - 1\})$
- $(\Gamma - 1, m_1, \{\Gamma - 1, u_1 - 1, u_2 - 1, \dots, u_{n-m_1-2} - 1\})$



Again using Prop. 4 (ii), we find the steady state probabilities of these states as  $\pi_{m_1+1}$  and  $\pi_{m_1}$ , respectively. Then, the steady state probability of  $S_1^{\mathbf{P}}$  is derived using the transition probabilities as:

$$\begin{aligned}\pi(S_1^{\mathbf{P}}) &= \pi_{m_1+1}(\tau_1(1-\tau_1)^{m_1} + \tau_1\tau_2[(1-\tau_1\tau_2)^{m_1} - (1-\tau_1)^{m_1}]) \\ &\quad + \pi_{m_1}(m_1\tau_1(1-\tau_1)^{m_1-1} - m_1\tau_1\tau_2[(1-\tau_1\tau_2)^{m_1-1} - (1-\tau_1)^{m_1-1}]) \\ &= \pi_{m_1}\end{aligned}\tag{56}$$

$\pi(S_2^{\mathbf{P}}) = \pi_{m_2}$  since there is a symmetry. The properties (i) and (ii) follow from Prop. 4 (i) and Property (iii) follows from (54).

The last case of ranges for the  $s$  value is  $\forall s \geq \Gamma$ . In order to show that the lemma still holds for this case, we will use induction. The preceding case  $s = \Gamma$  is the initial case and is already covered. Therefore, we assume that  $s > \Gamma$  and that the properties of the lemma holds for all the smaller values of  $s$ . Here we will again use two cases to make our analysis:

**Case 1.** If  $1 \notin \{u_1, u_2, \dots, u_{n-m-1}\}$

For the sake of readability, the probability expressions are shortened in the following way:

$$\pi_m^{(s)} = \pi(s, m, \{u_1, u_2, \dots, u_{n-m-1}\}) = \pi(S_1^{\mathbf{P}})\tag{57}$$

$$\pi_m^{(s-1)} = \pi(s-1, m, \{u_1-1, u_2-1, \dots, u_{n-m-1}-1\}) = \pi(Q_1^{\mathbf{P}})\tag{58}$$

$$\pi_{m-1}^{(s-1)} = \pi(s-1, m-1, \{\Gamma-1, u_1-1, u_2-1, \dots, u_{n-m-1}-1\})\tag{59}$$

A state of type  $(s, m, \{u_1, u_2, \dots, u_{n-m-1}\})$  can be preceded by states with probabilities  $\pi_m^{(s-1)}$  or  $\pi_{m-1}^{(s-1)}$ . Then, the value of  $\pi_m^{(s)}$  can be calculated using the transition probabilities as:

$$\pi_m^{(s)} = \pi_m^{(s-1)}(1 - (m+1)\tau_1(1-\tau_1)^m - (m+1)\tau_1\tau_2[(1-\tau_1\tau_2)^m - (1-\tau_1)^m])\tag{60}$$

$$+ \pi_{m-1}^{(s-1)}(m+1)(1 - m\tau_1(1-\tau_1)^{m-1} - m\tau_1\tau_2[(1-\tau_1\tau_2)^{m-1} - (1-\tau_1)^{m-1}])\tag{61}$$

Then,

$$\begin{aligned}
\lim_{n \rightarrow \infty} \frac{\pi_m^{(s)}}{\pi_m^{(s-1)}} &= \lim_{n \rightarrow \infty} \frac{\pi_m^{(s-1)}(1 - (m+1)\tau_1(1 - \tau_1)^m - (m+1)\tau_1\tau_2[(1 - \tau_1\tau_2)^m - (1 - \tau_1)^m])}{\pi_m^{(s-1)}} \\
&\quad + \frac{\pi_{m-1}^{(s-1)}(m+1)(1 - m\tau_1(1 - \tau_1)^{m-1} - m\tau_1\tau_2[(1 - \tau_1\tau_2)^{m-1} - (1 - \tau_1)^{m-1}])}{\pi_m^{(s-1)}} \\
&= \lim_{n \rightarrow \infty} 1 - (m+1)\tau_1(1 - \tau_1)^m - (m+1)\tau_1\tau_2[(1 - \tau_1\tau_2)^m - (1 - \tau_1)^m] \\
&\quad + \frac{\pi_{m-1}^{(s-1)}}{\pi_m^{(s-1)}}(m+1)(1 - m\tau_1(1 - \tau_1)^{m-1} - m\tau_1\tau_2[(1 - \tau_1\tau_2)^{m-1} - (1 - \tau_1)^{m-1}]) \\
&= \lim_{n \rightarrow \infty} 1 - \frac{m+1}{n}(n\tau_1)(1 - \tau_1)^m - \frac{m+1}{n}(n\tau_1)\tau_2[(1 - \tau_1\tau_2)^m - (1 - \tau_1)^m] \\
&\quad + \frac{n\pi_{m-1}^{(s-1)}}{\pi_m^{(s-1)}} \frac{m+1}{n} \left(1 - \frac{m}{n}(n\tau_1)(1 - \tau_1)^{m-1} - \frac{m}{n}(n\tau_1)\tau_2[(1 - \tau_1\tau_2)^{m-1} - (1 - \tau_1)^{m-1}]\right) \\
&\stackrel{(a)}{=} \lim_{n \rightarrow \infty} 1 - k\alpha e^{-k\alpha} - k\alpha\tau_2[e^{-\tau_2k\alpha} - e^{-k\alpha}] \\
&\quad + \frac{1}{\frac{1}{\alpha e^{-k\alpha} + \alpha\tau_2(e^{-\tau_2k\alpha} - e^{-k\alpha})} - k} k(1 - k\alpha e^{-k\alpha} - k\alpha\tau_2[e^{-\tau_2k\alpha} - e^{-k\alpha}]) = 1
\end{aligned} \tag{62}$$

where (a) follows from property (iii).

**Case 2.** If  $1 \in \{u_1, u_2, \dots, u_{n-m-1}\}$ , and without loss of generality we choose  $u_{n-m-1} = 1$

Again for the sake of readability, the probability expressions are shortened in the following

$$\pi_m^{(s)} = \pi(s, m, \{u_1, u_2, \dots, u_{n-m-2}, 1\}) = \pi(S_1^{\mathbf{P}})$$

way:  $\pi_m^{(s-1)} = \pi(s-1, m, \{\Gamma-1, u_1-1, u_2-1, \dots, u_{n-m-2}-1\}) = \pi(Q_1^{\mathbf{P}})$  A state of type

$$\pi_{m+1}^{(s-1)} = \pi(s-1, m+1, \{u_1-1, u_2-1, \dots, u_{n-m-2}-1\})$$

$(s, m, \{u_1, u_2, \dots, u_{n-m-2}, 1\})$  can be preceded by two types of states with steady state probabilities  $\pi_m^{(s-1)}$  and  $\pi_{m+1}^{(s-1)}$ . Then, using the transition probabilities, the value of  $\pi_m^{(s)}$  is obtained

as:

$$\pi_m^{(s)} = \pi_{m+1}^{(s-1)}(\tau_1(1 - \tau_1)^m + \tau_1\tau_2[(1 - \tau_1\tau_2)^m - (1 - \tau_1)^m]) \tag{63}$$

$$+ \pi_m^{(s-1)}(m\tau_1(1 - \tau_1)^{m-1} - m\tau_1\tau_2[(1 - \tau_1\tau_2)^{m-1} - (1 - \tau_1)^{m-1}]) \tag{64}$$

Then,

$$\begin{aligned}
\lim_{n \rightarrow \infty} \frac{\pi_m^{(s)}}{\pi_m^{(s-1)}} &= \lim_{n \rightarrow \infty} \frac{\pi_{m+1}^{(s-1)} (\tau_1 (1 - \tau_1)^m + \tau_1 \tau_2 [(1 - \tau_1 \tau_2)^m - (1 - \tau_1)^m])}{\pi_m^{(s-1)}} \\
&\quad + \frac{\pi_m^{(s-1)} (m \tau_1 (1 - \tau_1)^{m-1} - m \tau_1 \tau_2 [(1 - \tau_1 \tau_2)^{m-1} - (1 - \tau_1)^{m-1}])}{\pi_m^{(s-1)}} \\
&= \lim_{n \rightarrow \infty} \frac{\pi_{m+1}^{(s-1)}}{\pi_m^{(s-1)}} (\tau_1 (1 - \tau_1)^m + \tau_1 \tau_2 [(1 - \tau_1 \tau_2)^m - (1 - \tau_1)^m]) \\
&\quad + (m \tau_1 (1 - \tau_1)^{m-1} - m \tau_1 \tau_2 [(1 - \tau_1 \tau_2)^{m-1} - (1 - \tau_1)^{m-1}]) \\
&= \lim_{n \rightarrow \infty} \frac{\pi_{m+1}^{(s-1)}}{n \pi_m^{(s-1)}} ((n \tau_1) (1 - \tau_1)^m + (n \tau_1) \tau_2 [(1 - \tau_1 \tau_2)^m - (1 - \tau_1)^m]) \\
&\quad + \left( \frac{m}{n} (n \tau_1) (1 - \tau_1)^{m-1} - \frac{m}{n} (n \tau_1) \tau_2 [(1 - \tau_1 \tau_2)^{m-1} - (1 - \tau_1)^{m-1}] \right) \\
&= \lim_{n \rightarrow \infty} \left( \frac{1}{\alpha e^{-k\alpha} + \alpha \tau_2 (e^{-\tau_2 k\alpha} - e^{-k\alpha})} - k \right) (\alpha e^{-k\alpha} + \alpha \tau_2 [e^{-\tau_2 k\alpha} - e^{-k\alpha}]) \\
&\quad + (k \alpha e^{-k\alpha} - k \alpha \tau_2 [e^{-\tau_2 k\alpha} - e^{-k\alpha}]) = 1
\end{aligned} \tag{65}$$

With the last case, we completed the proof of property (i). Now, for the case  $m_1 = m_2$ ,

$$\begin{aligned}
\lim_{n \rightarrow \infty} \frac{\pi(S_1^{\mathbf{P}})}{\pi(S_2^{\mathbf{P}})} &= \lim_{n \rightarrow \infty} \frac{\pi(S_1^{\mathbf{P}}) \pi(Q_2^{\mathbf{P}}) \pi(Q_1^{\mathbf{P}})}{\pi(Q_1^{\mathbf{P}}) \pi(S_2^{\mathbf{P}}) \pi(Q_2^{\mathbf{P}})} \\
&\stackrel{(a)}{=} \lim_{n \rightarrow \infty} \frac{\pi(Q_1^{\mathbf{P}})}{\pi(Q_2^{\mathbf{P}})} \stackrel{(b)}{=} 1
\end{aligned} \tag{66}$$

Since the state of the pivot source for both the states  $Q_1^{\mathbf{P}}$  and  $Q_2^{\mathbf{P}}$  is  $s - 1$  and number of active sources is  $m_1$  and  $m_2$  respectively, (a) follows from property (i) and (b) follows from property (ii).

Similarly, for the case  $m_1 = m_2 + 1$ ,

$$\begin{aligned}
\lim_{n \rightarrow \infty} \frac{\pi(S_1^{\mathbf{P}})}{\pi(n S_2^{\mathbf{P}})} &= \lim_{n \rightarrow \infty} \frac{\pi(S_1^{\mathbf{P}}) \pi(Q_2^{\mathbf{P}}) \pi(Q_1^{\mathbf{P}})}{\pi(Q_1^{\mathbf{P}}) \pi(S_2^{\mathbf{P}}) n \pi(Q_2^{\mathbf{P}})} \\
&\stackrel{(a)}{=} \lim_{n \rightarrow \infty} \frac{\pi(Q_1^{\mathbf{P}})}{n \pi(Q_2^{\mathbf{P}})} \\
&\stackrel{(b)}{=} \frac{1}{\alpha e^{-k\alpha} + \alpha \tau_2 (e^{-\tau_2 k\alpha} - e^{-k\alpha})} - k
\end{aligned} \tag{67}$$

Since the state of the pivot source for both the states  $Q_1^{\mathbf{P}}$  and  $Q_2^{\mathbf{P}}$  is  $s - 1$  and number of active sources is  $m_1$  and  $m_2$  respectively, (a) follows from property (i) and (b) follows from property (iii).

#### ACKNOWLEDGMENT

The work in this paper has been funded in part by TUBITAK grants 117E215 and 119C028, and by Huawei.

## REFERENCES

- [1] E. Altman, R. E. Azouzi, D. S. Menasché, and Y. Xu, “Forever young: Aging control in dtns,” *CoRR*, vol. abs/1009.4733, 2010.
- [2] S. Kaul, R. Yates, and M. Gruteser, “Real-time status: How often should one update?,” in *Proc. IEEE INFOCOM*, pp. 2731–2735, IEEE, 2012.
- [3] Y. Sun, E. Uysal-Biyikoglu, R. D. Yates, C. E. Koksal, and N. B. Shroff, “Update or wait: How to keep your data fresh,” *IEEE Trans. Information Theory*, vol. 63, no. 11, pp. 7492–7508, 2017.
- [4] R. D. Yates and S. K. Kaul, “The age of information: Real-time status updating by multiple sources,” *IEEE Transactions on Information Theory*, vol. 65, no. 3, pp. 1807–1827, 2018.
- [5] M. Costa, M. Codreanu, and A. Ephremides, “Age of information with packet management,” *2014 IEEE International Symposium on Information Theory*, pp. 1583–1587, 2014.
- [6] Y. Inoue, H. Masuyama, T. Takine, and T. Tanaka, “A general formula for the stationary distribution of the age of information and its application to single-server queues,” *IEEE Transactions on Information Theory*, vol. 65, no. 12, pp. 8305–8324, 2019.
- [7] B. T. Bacinoglu, E. T. Ceran, and E. Uysal-Biyikoglu, “Age of information under energy replenishment constraints,” *2015 Information Theory and Applications Workshop (ITA)*, pp. 25–31, 2015.
- [8] L. Huang and E. Modiano, “Optimizing age-of-information in a multi-class queueing system,” *2015 IEEE International Symposium on Information Theory (ISIT)*, pp. 1681–1685, 2015.
- [9] A. Kosta, N. Pappas, A. Ephremides, and V. Angelakis, “Age and value of information: Non-linear age case,” *2017 IEEE International Symposium on Information Theory (ISIT)*, pp. 326–330, 2017.
- [10] R. D. Yates, E. Najm, E. Soljanin, and J. Zhong, “Timely updates over an erasure channel,” *2017 IEEE International Symposium on Information Theory (ISIT)*, pp. 316–320, 2017.
- [11] O. T. Yavascan and E. Uysal, “Analysis of slotted aloha with an age threshold,” *IEEE Journal on Selected Areas in Communications*, pp. 1–1, 2021. Early Access.
- [12] R. D. Yates and S. K. Kaul, “Status updates over unreliable multiaccess channels,” in *2017 IEEE International Symposium on Information Theory (ISIT)*, pp. 331–335, IEEE, 2017.

- [13] H. Chen, Y. Gu, and S.-C. Liew, “Age-of-information dependent random access for massive iot networks,” *preprint arXiv:2001.04780*, 2020.
- [14] X. Chen, K. Gatsis, H. Hassani, and S. S. Bidokhti, “Age of information in random access channels,” *arXiv preprint arXiv:1912.01473*, 2019.
- [15] D. C. Atabay, E. Uysal, and O. Kaya, “Improving age of information in random access channels,” in *Proc. AoI Workshop in conj. with IEEE INFOCOM*, July 2020.
- [16] Z. Jiang, B. Krishnamachari, X. Zheng, S. Zhou, and Z. Niu, “Timely status update in massive iot systems: Decentralized scheduling for wireless uplinks,” *arXiv preprint arXiv:1801.03975*, 2018.
- [17] O. T. Yavascan and E. Uysal, “Analysis of age-aware slotted aloha,” in *2020 IEEE Globecom Workshops (GC Wkshps)*, pp. 1–6, 2020.
- [18] A. Maatouk, M. Assaad, and A. Ephremides, “Minimizing the age of information in a csma environment,” *arXiv preprint arXiv:1901.00481*, 2019.
- [19] I. Kadota and E. Modiano, “Age of information in random access networks with stochastic arrivals,” *INFOCOM 2021, IEEE*, 2021.
- [20] Y. Sun, E. Uysal-Biyikoglu, R. D. Yates, C. E. Koksall, and N. B. Shroff, “Update or wait: How to keep your data fresh,” *IEEE Trans. on Info. Theory*, vol. 63, no. 11, pp. 7492–7508, 2017.
- [21] G. Liva, “Graph-based analysis and optimization of contention resolution diversity slotted aloha,” *IEEE Trans. on Communications*, vol. 59, no. 2, pp. 477–487, 2010.